

Specificity in Inhibitory Systems Associated with Prefrontal Pathways to Temporal Cortex in Primates

M. Medalla¹, P. Lera², M. Feinberg¹ and H. Barbas^{1,3}

¹Departments of Health Sciences, ²Cognitive and Neural Systems and ³Program in Neuroscience, Boston University and School of Medicine, Boston, MA, USA

The prefrontal cortex selects relevant signals and suppresses irrelevant stimuli for a given task through mechanisms that are not understood. We addressed this issue using as a model system the pathways from the functionally distinct prefrontal areas 10 and 32 to auditory association cortex, and investigated their relationship to inhibitory neurons labeled for calbindin (CB) or parvalbumin (PV), which differ in mode of inhibition. Projection neurons in area 10 originated mostly in layers 2–3 and were intermingled with CB inhibitory neurons. In contrast, projections from area 32 originated predominantly in layers 5–6 among PV inhibitory neurons. Prefrontal axonal boutons terminating in layers 2–3 of auditory association cortex were larger than those terminating in layer 1. Most prefrontal axons synapsed on spines of excitatory neurons but a significant number targeted dendritic shafts of inhibitory neurons. Axons from area 10 targeted CB and PV inhibitory neurons, whereas axons from area 32 targeted PV inhibitory neurons. The preferential association of the 2 prefrontal pathways with distinct classes of inhibitory neurons at their origin and termination may reflect the specialization of area 10 in working memory functions and area 32 in emotional communication. These findings suggest diversity in inhibitory control by distinct prefrontal pathways.

Keywords: auditory association cortex, calbindin, inhibitory neurons, laminar connections, parvalbumin

Introduction

At any one time large arrays of stimuli impinge on our senses, yet we can engage in complex tasks, such as following a conversation in a noisy environment. The prefrontal cortex is necessary for this remarkable ability (reviewed in Dagenbach and Carr 1994; Posner and DiGirolamo 1998), exemplified in patients with damage to lateral prefrontal cortex who are impaired in auditory tasks when irrelevant auditory stimuli are introduced. The performance of these patients is correlated with decreased neural activity in dorsolateral prefrontal areas and a concomitant increase of activity in auditory cortices (Chao and Knight 1998). Similarly, in pathological aging in humans, neural changes in prefrontal cortices diminish inhibitory influences in temporal auditory areas, impairing the ability to ignore irrelevant sounds (Woods and Knight 1986).

The mechanism of selection or inhibition of information by prefrontal cortex is not understood. Selection is likely mediated by pyramidal neurons which project through glutamatergic pathways to other areas. Inhibition in the cortex is mediated largely through GABAergic (gamma-amino butyric acidergic) neurons that comprise a diverse group distinguished by phenotype, the profiles of neurons they synapse with, and efficacy in inhibitory control (e.g., Gupta et al. 2000; reviewed in White and Keller 1989; Kawaguchi and Kubota 1997; Thomson and Deuchars 1997; Somogyi et al. 1998). A useful classification of

inhibitory neurons in the cortex is by their expression of the calcium binding proteins parvalbumin (PV), calbindin (CB), and calretinin (CR), which comprise largely nonoverlapping groups of inhibitory neurons in the primate cortex (e.g., Hendry et al. 1989; DeFelipe 1997). CR neurons are found mostly in the upper layers (2–3a), and innervate mostly other GABAergic neurons (Meskenaitė 1997; DeFelipe et al. 1999; Gonchar and Burkhalter 1999; Melchitzky et al. 2005). PV and CB neurons are distinguished by significant differences. PV is expressed in basket and chandelier inhibitory neurons, which are found mainly in the middle layers of the cortex, and synapse with pyramidal cell bodies, proximal dendrites, and axon initial segments (e.g., Somogyi et al. 1983; DeFelipe et al. 1989b; reviewed in Kawaguchi and Kubota 1997; Somogyi et al. 1998). CB is expressed mainly in inhibitory double bouquet neurons in the cortex, which are most densely distributed in cortical layers 2 and 3, and innervate distal dendrites and spines of other neurons (e.g., DeFelipe et al. 1989a; Peters and Sethares 1997; Zaitsev et al. 2005).

Inhibitory neurons in primates act over short distances at the columnar or intercolumnar level, a feature they share with some excitatory neurons (e.g., Kritzer et al. 1992; Melchitzky et al. 1998; Rao et al. 1999; Constantinidis et al. 2001; Krimer and Goldman-Rakic 2001; Constantinidis et al. 2002). However, excitatory neurons also act through pathways that leave the gray matter and travel in the white matter over short or long distances. The prefrontal cortex participates in an extensive network of such connections, and may exercise excitatory and inhibitory control by synapsing, respectively, with excitatory and inhibitory neurons in other cortices. Alternatively, excitation and inhibition may be mediated intrinsically within prefrontal cortex, allowing some messages to reach other areas, and blocking others.

Here we addressed these issues by investigating the organization of projections to temporal auditory association cortex from 2 prefrontal areas, cingulate area 32, and frontal polar area 10. Both areas have strong connections with superior temporal auditory association areas, but otherwise have different functional attributes (reviewed in Barbas et al. 2002). Area 32 has a role in emotional communication (reviewed in Vogt and Barbas 1988; Paus 2001) and a demonstrated role in inhibitory control of superior temporal cortex (Müller-Preuss and Ploog 1981). Area 10 has a role in a specific type of working memory (Koechlin et al. 1999, 2003), but its role in inhibitory control is unknown. We compared the relationship of projection neurons from these functionally distinct areas with the neurochemical classes of local inhibitory neurons labeled by PV or CB at the sites of origin in prefrontal cortex, and termination of their axons in layers 1 and 2–3 of auditory association cortex.

We provide novel evidence suggesting a distinct mode of inhibitory control by these functionally distinct prefrontal pathways on temporal auditory association cortex.

Methods

Subjects

Animals were obtained from the New England Primate Research Center (NEPRC). Experiments were conducted according to the NIH guide for the Care and Use of Laboratory Animals (DHEW Publication no. [National Institutes of Health, NIH] 80-22, revised 1987, Office of Science and Health Reports, DRR/NIH, Bethesda, MD), and protocols were approved by the Institutional Animal Care and Use Committee at NEPRC, Harvard Medical School, and Boston University School of Medicine.

Experiments were conducted on 5 rhesus monkeys (*Macaca mulatta*) of both sexes, 2–3 years of age grouped by the tracer injection site in temporal or prefrontal cortices, with a total of 7 injection sites as follows: tracer injection in superior temporal cortex: case Bjb (female, 2 years; left hemisphere, fast blue [FB]); case BCr (male, 3 years, right hemisphere, fluororuby [FR]); case AV (left hemisphere, biotinylated dextran amine [BDA]). Tracer injection in area 10: case BF (female, 2 years; left hemisphere, BDA); case BC (left hemisphere, BDA). Tracer injection in area 32: case Ble (female, 3 years; right hemisphere, fluoroemerald [FE]); case BI (right hemisphere, BDA).

Surgical Procedures

The monkeys were anesthetized with ketamine hydrochloride (10–15 mg/kg, intramuscularly) followed by isoflurane anesthetic until a surgical level of anesthesia was accomplished. The monkeys were then placed in a stereotaxic apparatus and a small region of the superior temporal or prefrontal cortex was exposed. Surgery was performed under aseptic conditions, while heart rate, muscle tone, respiration, and pupillary dilatation were closely monitored.

Injection of Neural Tracers

Injections of retrograde or bidirectional tracers were placed in superior temporal areas Ts1–Ts2 in 3 different animals (Fig. 1). In one case (Bjb), we injected 1.5 μ L of the retrograde tracer FB (Polysciences Inc., Warrington, PA) diluted to a concentration of 5 mg/mL. In 2 cases a 1:1 mixture of the 10 000 and 3000 MW forms of bidirectional tracers, BDA (case AV; biotinylated dextran amine, Molecular Probes, Eugene, OR), or FR (case BCr; dextran tetramethylrhodamine, Molecular Probes) was injected to optimize anterograde and retrograde labeling. The dyes were diluted to a concentration of 10 mg/mL and were injected in volumes of 1.5 μ L (for BDA, case AV) and 4 μ L (for FR, case BCr).

Injections of BDA were placed in prefrontal areas 10 (cases BC and BF) and 32 (case BI) in 3 animals (Fig. 1). In case BI we also injected the tracer fluoroemerald FE (case Ble; dextran fluorescein, Molecular Probes) in area 32. The dyes were diluted to a concentration of 10 mg/mL and were injected in volumes of 3–4 μ L (cases BI and Ble) and 8–10 μ L (cases BC and BF). We used the 10 000 MW form of BDA and FE, known to be optimal for anterograde but not retrograde labeling (e.g., Veenman et al. 1992; Reiner et al. 2000; and personal observations). This form of dextran amine labels the entire extent of axon terminals and boutons.

In each case the dye was delivered in 2–4 penetrations at a depth of 1.2–1.6 mm below the pial surface. For each injection the needle was left in situ for 10–15 min to allow local diffusion of the dye at the injection site and prevent upward suction of the dye upon retraction of the needle.

Perfusion and Tissue Processing

The survival period was 18 days. The animals were then anesthetized with a lethal dose of sodium pentobarbital (>50 mg/kg, to effect) and perfused with 4% paraformaldehyde (case AV), or 4% paraformaldehyde and 0.2% glutaraldehyde (all other cases) in 0.1 M phosphate buffer (PB, pH 7.4). The brain was removed from the skull, photographed, and placed in graded solutions of sucrose (10–30% in 0.1 M PB) for cryoprotection.

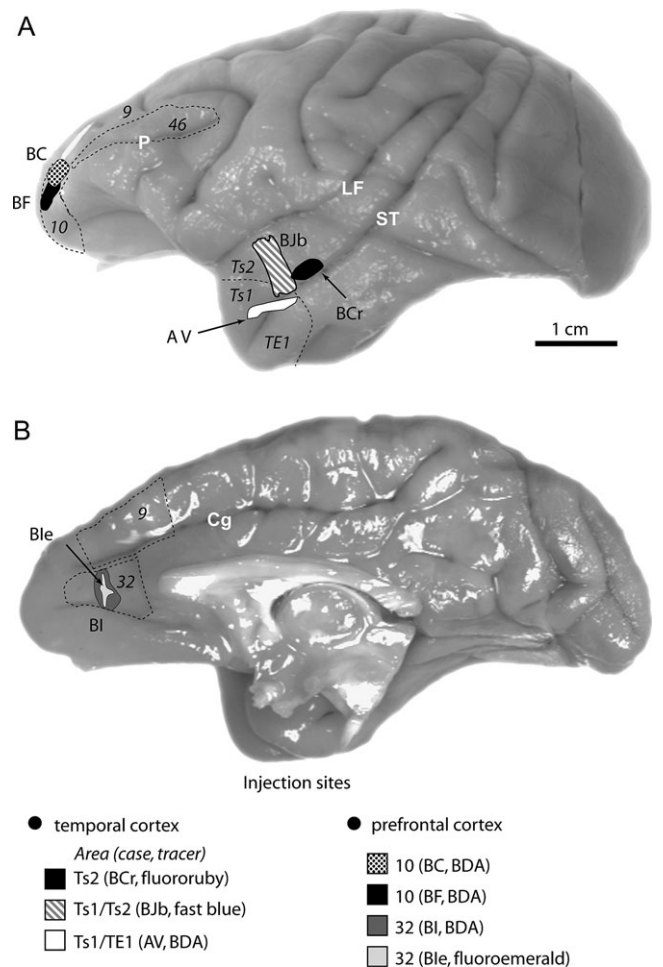


Figure 1. The injection sites of bidirectional or retrograde tracers. (A) Photograph of the lateral surface of a rhesus monkey brain showing the injection sites in superior temporal cortices (cases AV, Bjb, BCr), and in prefrontal area 10 (cases BC and BF). (B) Photograph of the medial surface showing the injection sites in area 32 (cases Ble and BI). Abbreviations: Cg, cingulate sulcus; LF, lateral fissure; P, principal sulcus; ST, superior temporal sulcus.

Brains were frozen in -75°C isopentane (Fisher, Waltham, MA) according to the protocol of Rosene et al. (1986), and cut on a freezing microtome in the coronal plane at 50 μ m to produce 10 series per hemisphere. In cases with injection of fluorescent retrograde or bidirectional tracers in superior temporal cortex, 2 series of sections were mounted on gelatin-coated glass slides immediately after cutting, dried, and placed in cold storage (4°C) until plotting of labeled neurons, as described previously (e.g., Barbas 1995; Barbas et al. 2005a).

Tissue Processing for Light and Fluorescence Microscopy

For all tissue processing, free-floating sections were washed (3×10 min, under slow agitation, 4°C) with 0.01 M phosphate-buffered saline (PBS, pH 7.4) and incubated in 50 mM glycine for 1 h prior to processing. To view BDA label, brain sections were rinsed in PBS and incubated for 1 h in an avidin-biotin (AB) horse radish peroxidase (HRP) complex (Vectastain PK-6100 ABC Elite kit, Vector Laboratories, Burlingame, CA), diluted 1:100 in PBS with 0.1% Triton X-100 (Sigma, St Louis, MO). The sections were then washed and processed for 2–3 min for immunoperoxidase reaction using diaminobenzidine (DAB kit, Zymed Laboratories Inc., South San Francisco, CA).

In the cases with injections of fluorescent tracers (FE and FR), we used antibodies against the fluorophore to convert the fluorescent label to DAB reaction product and visualize label using brightfield or electron microscopy (EM). For the FE case (Ble), where there was an injection of

BDA in the same animal, sections were incubated in AB blocking reagent (AB blocking kit, Vector Labs), to prevent cross-reaction with BDA. Sections were rinsed and preblocked for 1 h in 5% normal goat serum (NGS, Vector Labs) and 5% bovine serum albumin (BSA, Sigma) with Triton-X (0.2% for brightfield tissue; 0.025% for EM tissue). Sections were incubated overnight in the primary antibody for either FE or FR (1:800, rabbit polyclonal; Molecular Probes) diluted in PBS with 1% NGS, 1% BSA, and 0.1% Triton-X (0.025% for EM tissue). After rinsing, sections were incubated for 2 h in biotinylated goat anti-rabbit IgG (1:200; Vector Labs). Subsequently, sections were incubated in AB-HRP solution and processed for DAB, as described above. Sections for brightfield analysis were rinsed in PB, mounted on gelatin-coated glass slides, and dried. Every other section was counterstained with thionin (Sigma), and sections were coverslipped with Entellan (EMD Chemicals, Gibbstown, NJ). In some sections FE labeling was visualized using the peroxidase-antiperoxidase (PAP) method, which does not involve biotinylated secondary antibodies (Zikopoulos and Barbas 2006). Labeling using the PAP method was similar to labeling after processing with AB.

For viewing large areas with tracer label under fluorescence illumination along with distinct neurochemical classes of inhibitory interneurons, sections were incubated overnight in the primary antibody for either CB (1:2000, mouse monoclonal; Swant, Bellinzona, Switzerland) or PV (1:2000, mouse monoclonal; Chemicon, Temecula, CA). Sections were then incubated overnight in goat anti-mouse IgG conjugated with the fluorescent probe Alexa 488 (1:200, with 1% NGS, 1% BSA, and 0.1% Triton-X in PBS; Molecular Probes), rinsed in PB, mounted, dried, and coverslipped with Krystalon (EMD Chemicals).

Tissue Processing for EM

For viewing prefrontal pathways labeled with tracers and CB or PV postsynaptic sites in superior temporal cortex at the electron microscope we employed preembedding immunohistochemistry of gold-conjugated secondary antibodies. Sections were processed for BDA to label prefrontal pathways, and then preblocked using reduced amounts of Triton-X (0.025%; as described above). The tissue was then incubated overnight in the primary antibody for either PV (1:2000; mouse monoclonal, Chemicon; or rabbit polyclonal, Swant) or CB (1:2000; mouse monoclonal, Swant). After rinsing, sections were incubated overnight in gold-conjugated goat anti-mouse or anti-rabbit IgG (gold particle diameter, 1 nm; diluted 1:50 in PBS with 1% NGS, 1% BSA, and 0.1% gelatin; Amersham Biosciences, Piscataway, NJ). To prevent diffusion of the gold particles, the tissue was postfixed with 2% or 6% glutaraldehyde, either for 1 h at room temperature or using a conventional 650-W microwave oven (Sharp Electronics Corp., Mahwah, NJ) for up to ~30 s until the fixative temperature reached ~35 °C, as described (Jensen and Harris 1989; Giberson and Elliott 2001). After rinsing sections in PBS and distilled water, gold labeling was intensified using a silver enhancement kit (6- to 12-min incubation; IntenSE M kit, Amersham Biosciences).

For triple labeling, we combined DAB and gold staining with tetramethylbenzidine (TMB) staining, which precipitates HRP into rod-shaped crystals that are easily discernible from the dark flocculent DAB precipitate and the bead-like gold particles. After the DAB precipitation of BDA or FE-labeled fibers from prefrontal pathways (as above), sections were incubated in AB blocking reagent (Vector Labs), to prevent cross-reaction with the subsequent TMB procedure. For BDA-labeled tissue (case BI), sections were cocubated overnight in both primary antibodies for PV (rabbit polyclonal) and CB (mouse monoclonal), and then for 2 h in biotinylated anti-mouse IgG, followed by 1 h in AB-HRP (as above). For tissue labeled with the tracer FE (case BIE), we used 2 mouse monoclonal primary antibodies for PV and CB, processed successively. We used the Mouse-on-Mouse blocking kit (M.O.M. basic kit, Vector Labs) between incubations, specifically after the incubation in biotinylated anti-mouse IgG, to prevent cross-reaction between the 2 mouse monoclonal antibodies. After binding of the biotinylated secondary antibodies and AB-HRP, sections were incubated overnight in the appropriate gold-conjugated IgG, as described above. After postfixation, silver intensification of gold, and rinses in distilled water (2 × 5 min), sections were processed for immunoperoxidase reaction with TMB (5–15 min incubation; 0.005% TMB dissolved in 100% ethanol, 5% ammonium paratungstate, 0.004% NH₄Cl, 0.005% H₂O₂; in 0.1 M PB, pH 6) as described (Gonchar and Burkhalter 2003). For

additional stabilization and intensification of the TMB reaction product, sections were treated for 7–10 min in a DAB-cobalt chloride (CoCl) solution (0.05% DAB, 0.02% CoCl, 0.004% NH₄Cl, 0.005% H₂O₂; in 0.1 M PB, pH 6), modified from previous studies (Gonchar and Burkhalter 2003; Moore et al. 2004). The presence of TMB crystals in DAB tracer-labeled boutons was not observed, indicating that the AB blocking step prevented cross-reaction between the tracer (BDA or FE) and PV or CB. There was no colocalization of gold and TMB label, indicating that the M.O.M. blocking step effectively prevented cross-reaction between CB and PV mouse monoclonal antibodies.

To rule out the possibility of nonspecific immunoreactivity, control experiments were performed, with sections matched to those described above, where the primary antibodies were omitted but all other steps were identical to the experimental conditions. To test the efficacy of blocking agents, control tissue sections were processed with the blocking reagents prior to AB-HRP binding (for AB blocking kit) or between primary and secondary antibody incubations (for M.O.M. kit). In all control experiments there was no immunohistochemical labeling.

After immunohistochemical procedures tissue sections were mounted on glass slides and quickly viewed under the light microscope and images were captured with a CCD camera. Small blocks of sections with anterograde and PV and/or CB label were cut under a dissecting microscope and rinsed thoroughly in 0.1 M PB. Sections were then postfixed in 2 stages: first in 1% osmium tetroxide (Ted Pella, Inc., Redding, CA) with 1.5% potassium ferrocyanide (Sigma) in PB for 30 min, and second in 1% osmium tetroxide in PB for 15–20 min. After rinses in PB and then distilled water, sections were dehydrated in 50% alcohol and then stained with 1% uranyl acetate (Electron Microscopy Sciences, Hatfield, PA) in 70% alcohol for 30 min. Dehydration of the sections was then continued in an ascending series of alcohols (90%, 95%, 100%). Subsequently, sections were infiltrated with 100% propylene oxide (Electron Microscopy Sciences) and then a 1:1 mixture of propylene oxide and araldite resin (Earnest F. Fullam, Inc., Latham, NY). Sections were placed overnight in 100% araldite under a vacuum desiccator, then flat embedded in aclar (Ted Pella), and cured for 48 h at 60 °C. Pieces of aclar-embedded tissue then were cut and re-embedded in araldite blocks. Serial ultrathin sections (50 nm) were cut with a diamond knife (Diatome, Fort Washington, PA) using an ultramicrotome (Ultracut; Leica, Wein, Austria) and collected on single slot pioloform-coated grids. Depending on the contrast of the tissue, some sections were counterstained with 3% uranyl acetate and Reynolds lead citrate (Ted Pella).

Data Analysis

Mapping Projection Neurons

Coronal sections in one series (representing 1 in 10 sections) ipsilateral to the injection site were viewed under brightfield or fluorescence illumination (200×) to map retrogradely labeled neurons in the prefrontal cortex in cases with tracer injections in temporal cortex. We placed areal and laminar boundaries from Nissl-stained coronal sections, based on the architectonic map of Barbas and Pandya (1989). We traced areas of interest and plotted labeled neurons using a microscope (Olympus BX51, Olympus America, Inc., Center Valley, PA) coupled to a commercial computer-software system (NeuroLucida, MicroBrightfield, Williston, VT). We conducted exhaustive sampling through the prefrontal cortex and counted all labeled neurons by area and layer in one series of sections. In areas with significant label (>20 neurons), we expressed the number of labeled neurons in an area as a percentage of the total number in all prefrontal areas. The laminar distributions of labeled neurons were expressed as the percentage in the upper (2–3) and deep (5–6) layers of the total number of projection neurons in each area.

Mapping Labeled Synapses

To map the synapses formed by prefrontal axons onto temporal cortex, pieces of aclar-embedded tissue with label in temporal cortex were cut from superficial layer 1, which is largely cell-free and extends to about 150–200 μm below the pial surface. Pieces of tissue from layers 2–3 of temporal cortex were cut starting ~80 μm below the border of layers 1

and 2 and extending to ~380 μm , to include the bottom part of layer 2 and the top part of layer 3. For each case and each set of immunolabeling, we cut 1–2 pieces of tissue (total = 13 in 4 cases) from each layer and re-embedded them in blocks for serial sectioning. Blocks of tissue from layer 1 were trimmed to an average of 110 \times 220 μm and for layers 2–3 to an average of 130 \times 360 μm .

Ultrathin sections (unstained or grid-stained) were examined at 60 kV with a transmission electron microscope (100CX; Jeol, Peabody, MA). Labeled boutons from prefrontal cortex terminating onto postsynaptic elements in temporal cortex were photographed at 10 000 \times or 6500 \times , and the negatives were scanned (Epson Perfection 4990 Photo Scanner, Epson America, Inc., Long Beach, CA). Exhaustive sampling of labeled boutons was conducted from an average of 280 sections from each piece of tissue through layer 1, and from an average of 270 sections through layers 2–3. Data were collected systematically and exhaustively to yield a comparable sample of labeled boutons from each layer.

Serial Reconstruction of Synapses

We used the freeware program Reconstruct (www.synapses.bu.edu; Fiala 2005) to analyze labeled boutons and their postsynaptic targets in a series of 30–50 sections. We used the program to correct for the misalignments between images of sections caused by serial sectioning and scanning of the tissue (Fiala and Harris 2002). The dimensions of the scanned images were calculated by comparison with an image of a diffraction grating. The thickness of the imaged sections was estimated using the method of cylindrical diameters (Fiala and Harris 2001). After calibration, object contours of boutons and postsynaptic elements were manually traced section-by-section, and used to calculate volume and surface area. The program was used to generate a 3-dimensional (3D) model (Virtual Reality Modeling Language), which was imported in 3D Studio Max (v 2.5, Autodesk Inc., San Rafael, CA) for additional rendering.

Statistics

Data sets were compared using analysis of variance (ANOVA) and Bonferroni's post hoc test in either Statistica (v.7 for Windows, StatSoft Inc., Tulsa, OK) or Matlab Statistics Toolbox (The Mathworks, Inc., Natick, MA). Linear regression was conducted using least-squares approximation in Matlab. In each case a significance level of $P < 0.05$ was used.

Photography

Photomicrographs of overlapping populations of tracer-labeled projection neurons and CB+ or PV+ inhibitory interneurons in prefrontal areas were captured with a CCD camera (Olympus DP70) mounted on a microscope (Olympus BX51) and connected to a PC computer. This method was used to capture images obtained under light or fluorescence illumination. We acquired image stacks of several focal planes in each area of interest and created pictures of 50- μm -thick sections focused throughout their z-axis extent using ImageJ (v. 1.32j for Windows, NIH, USA) as described previously (Zikopoulos and Barbas 2006). To show the pattern of label, we obtained separate photomicrographs of distinct sites throughout the entire depth of the cortex at 200 \times and manually stitched the images to create a montage. Images from matched tissue sections were superimposed to highlight the relative distribution of labeled projection neurons and inhibitory interneurons. Photomicrographs of EM images were prepared directly from the scanned images. Figures were prepared with Adobe Photoshop (Adobe Systems Inc., San Jose, CA) and overall brightness and contrast were adjusted without retouching.

Results

Origin of Prefrontal Projection Neurons Directed to Superior Temporal Cortex: Light and Fluorescence Microscopy

Data on prefrontal projection neurons directed to temporal cortices were obtained from 3 distinct injection sites in superior temporal auditory association areas (areas Ts1–Ts2)

known to be strongly connected with several prefrontal areas (reviewed in Barbas 1992). The most caudal injection was located within area Ts2 (case BCr), extending from the fundus of the superior temporal sulcus to the ventral third of the superior temporal gyrus (Fig. 1). One injection was situated at the border of areas Ts1 and Ts2 but penetrated only the superficial layers (1–3), and covered the ventral-caudal part of area Ts1 and extended dorsally into area Ts2 (case BJB). The third injection spanned the ventral part of area Ts1 (case AV); it extended within the banks of the superior temporal sulcus, and impinged on the dorsolateral part of inferior temporal visual area TE1.

Topography of Prefrontal Projections to Superior Temporal Cortex

Quantitative analysis throughout the prefrontal cortex revealed that most projection neurons directed to superior temporal cortex arose from areas 10, 32, 25, and 14 (cases AV and BCr; Fig. 2), consistent with previous studies (Barbas and Mesulam 1985; Petrides and Pandya 1988; Barbas et al. 1999; Hackett et al. 1999; Romanski et al. 1999). In particular, area 10 in the frontal pole and medial areas in the anterior cingulate issued the strongest projections to superior temporal cortex. Significant numbers of labeled neurons were also found in the anterior parts of dorso-lateral areas 9 and 46d (Fig. 2C,D), in posterior orbitofrontal areas 11, 13, OPall, and OPro (Fig. 2E,F) and ventrolateral areas 12 and 46v (case AV, not shown). Below we focus in more detail on the connections of areas 10 and 32 with temporal auditory association cortex.

The highest concentrations of projection neurons were found in area 10 (Fig. 2A,B,G), originating in its entire rostro-caudal and medio-dorsal extent (Figs. 2A,B and 3). However, the distribution of labeled neurons originating from the dorsal, medial, and ventral subregions of area 10 varied depending on the specific area of termination in superior temporal cortex (Fig. 3). The dorsal part of area 10 issued the strongest projections to area Ts2 (Fig. 3, case BCr), and medial area 10 issued strong projections to the anterior part of area Ts2, extending to posterior area Ts1 (Fig. 3, case BJB). Significant numbers of projection neurons originated from ventral area 10 and projected to anterior and ventral area Ts1, and possibly to area TE1, based on the extent of the injection site (Fig. 3, case AV).

Area 32 in the anterior cingulate also projected robustly to superior temporal cortices. Area 32 does not have subareas like area 10, and the distribution of projection neurons was similar among cases. Projection neurons were found along the entire rostro-caudal and dorso-ventral extent of area 32, and were especially concentrated in its ventral gyral parts (Fig. 2D,E).

Laminar Origin of Projection Neurons in Areas 10 and 32 and their Relationship to Local Inhibitory Neurons Labeled with CB or PV

Quantitative data on the laminar origin of projection neurons from prefrontal areas 10 and 32 were obtained from 3 cases (AV, BCr, and BJB). As shown in Figure 4, projection neurons directed to superior temporal cortices differed dramatically in laminar origin, found predominantly in the deep layers (5–6) of area 32 (77%), and mostly in the upper layers (2–3) of area 10 (75%; ANOVA, $P < 0.02$). Among the subregions of area 10, the dorsal part issued the highest proportion of projection neurons from the upper layers. The laminar pattern of projections from areas 10 and 32 was consistent across cases (Fig. 4), including

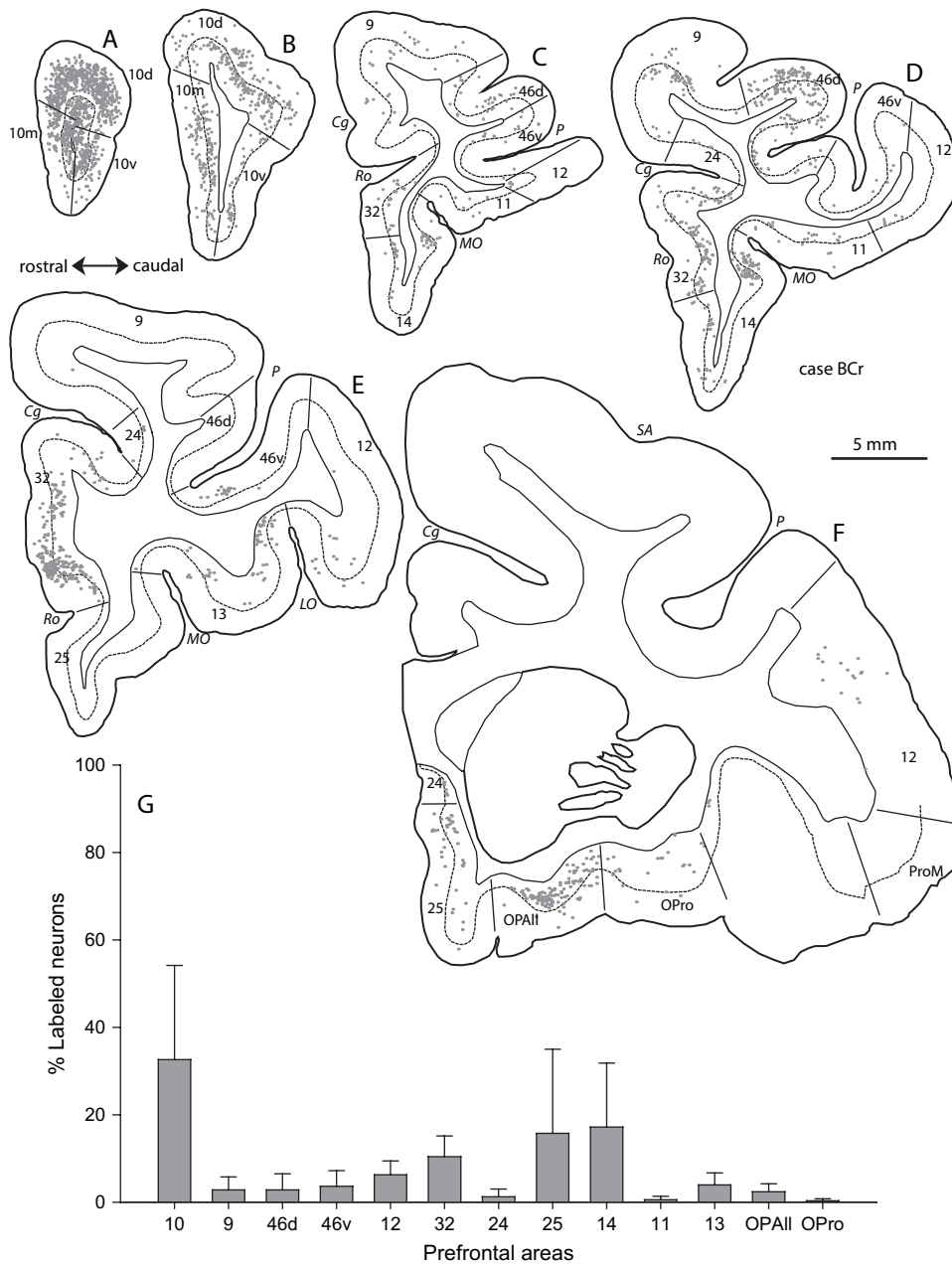


Figure 2. Distribution of projection neurons in prefrontal cortices directed to superior temporal cortices. (A–F) Coronal sections of rostral (A) through caudal (F) levels of the prefrontal cortex, showing the distribution of projection neurons (gray dots) in prefrontal cortices directed to superior temporal cortices in a case with injection of the bidirectional tracer fluororuby in superior temporal cortex (case BCr). The dotted line through the cortex shows the upper boundary of layer 5. Vertical lines through the cortex show the boundaries of architectonic areas. Abbreviations: Cg, cingulate sulcus; LO, lateral orbital sulcus; MO, medial orbital sulcus; OPAII, orbital periallocortex; OPro, orbital proisocortex; P, principal sulcus; ProM, promotor cortex; Ro, rostral sulcus; SA, superior limb of the arcuate sulcus. (G) Histogram showing the average distribution of projection neurons in prefrontal cortices after injection of tracers in superior temporal cortices. The sum of all bars is 100%. Vertical lines show standard deviation.

the case in which the core of the injection was mainly in layers 1–3 of areas Ts1–2 (case Bjb).

The marked contrast in the laminar organization of projection neurons in area 10 and area 32 placed these populations in different microenvironments with respect to 2 neurochemical classes of local inhibitory neurons. The predominant populations of projection neurons in the upper layers (2–3) of area 10 were intermingled mostly with the cell bodies and processes of CB+ interneurons, which are also prevalent in layers 2–3a (Fig. 5A,B). In contrast, projection neurons from area 32, which were most densely distributed in the deep layers

(5–6), were mostly intermingled with PV+ interneurons, which are prevalent in the middle to deep layers (Fig. 5C,D). As noted in a previous study (Dombrowski et al. 2001) and confirmed here, PV+ neurons and processes in area 32, were closely apposed to the cell bodies of pyramidal neurons in layers 5–6. The synaptic interactions of projection neurons from areas 10 and 32 with local inhibitory neurons are not known. Nevertheless, the findings show 2 distinct populations of outputs directed to superior temporal cortex emanating preferentially from laminar microenvironments dominated by specific neurochemical classes of inhibitory neurons.

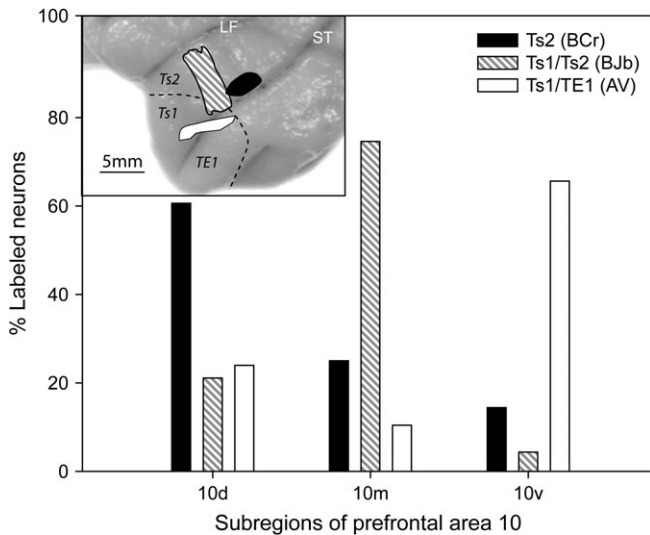


Figure 3. Topography of projection neurons in dorsal, medial, and ventral parts of area 10 directed to superior temporal areas. Inset (top, left) shows the injection sites in superior temporal cortex. Bars representing projection to each injection site add up to 100%. Abbreviations are as in Figure 1.

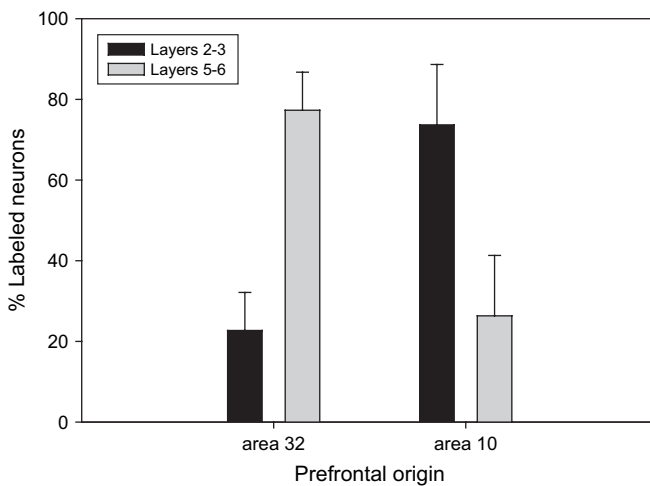


Figure 4. Laminar origin of prefrontal projection neurons. Normalized data from 3 cases showing the distribution of projection neurons in layers 2–3 (black bars) and in layers 5–6 (gray bars) of areas 32 and 10 directed to superior temporal cortices. The pairs of bars for each area add up to 100%. Vertical lines show standard error.

Terminations of Prefrontal Axons in Superior Temporal Cortex: EM

The injection sites in prefrontal areas 10 and 32 are shown in Figure 1. Two injections of BDA (cases BC and BF) were situated in the caudal and dorsal part of area 10; one included a small part of rostral area 9 (case BC). Two distinct injections in one animal were situated in the central portion of area 32 (cases BI, BDA; and BIE, fluoroemerald). Both injection sites spanned the entire dorso-ventral extent of area 32, but in one, the core of the injection was concentrated in layers 4–6 (case BIE). The findings from the 2 injection sites were similar.

Prefrontal axons from areas 10 and 32 terminated robustly in superior temporal cortex, especially in auditory association areas Ts1–Ts2, where labeled terminations were found in all layers, consistent with quantitative data from a previous study

(Barbas et al. 2005b). Here, we used serial uninterrupted sections to identify and characterize synapses from axons originating in prefrontal areas 10 ($n = 155$) and 32 ($n = 75$), and terminating in layers 1 and 2–3 of superior temporal area Ts1 from 4 injection sites (cases BC, BF, BI, and BIE). We reconstructed in 3D the majority of these boutons ($n = 138$ from area 10; $n = 55$ from area 32) to assess and compare their ultrastructural features.

Structural Features of Prefrontal Pathways and their Synaptic Targets in Temporal Cortex

Boutons originating from area 10 ($n = 71$) had a comparable volume ($0.2 \pm 0.01 \mu\text{m}^3$) to boutons originating from area 32 ($n = 30$; volume, $0.21 \pm 0.02 \mu\text{m}^3$; ANOVA, $P > 0.05$) in layer 1 of superior temporal area Ts1 (Figs. 6A–C and 7E,H–I). Similarly, in layers 2–3 of Ts1, boutons from axons originating in area 10 ($n = 67$) had a comparable volume ($0.28 \pm 0.02 \mu\text{m}^3$) as boutons from area 32 ($n = 25$; volume, $0.29 \pm 0.03 \mu\text{m}^3$; $P > 0.05$; Figs. 6A–C and 7F–G). However, the population of boutons terminating in layer 1 of superior temporal cortex differed significantly in size from boutons terminating in layers 2–3, regardless of their origin in areas 32 or 10 ($P < 0.001$; Figs. 6C and 7E–I). We combined these results with data from a previous study (Germuska et al. 2006), and found that boutons from area 10 were increasingly larger when terminating in layers 1 through 4–5 (ANOVA, $P \ll 0.001$; Bonferroni, $P < 0.01$ for all pairs; Fig. 6C). The volumes of boutons in layer 1 obtained from the 2 studies did not differ significantly (Bonferroni, $P = 0.45$).

There was a linear relationship between bouton volume and spine volume ($R^2 = 0.35$, $P \ll 0.001$; Fig. 6D), between bouton volume and postsynaptic density (PSD) area ($R^2 = 0.42$, $P \ll 0.001$; Fig. 6E), and between spine volume and PSD area ($R^2 = 0.57$, $P \ll 0.001$; Fig. 6F), confirming and extending previous findings (Germuska et al. 2006). The above relationships were consistent for areas 32 and 10 and layers 1 and 2–3, so the data were pooled.

Synapses of Prefrontal Pathways with Excitatory and Inhibitory Neurons in Temporal Cortex

We then determined the extent of the excitatory and inhibitory postsynaptic targets in superior temporal cortex from the subset of axonal boutons from area 10 ($n = 114$) and area 32 ($n = 70$) that formed identifiable synapses in temporal cortex. We used morphological criteria (for review see Peters et al. 1991) to classify the postsynaptic targets of labeled boutons as either spiny dendrites, which belong to excitatory neurons (Fig. 7B,E,F,H,I), or aspiny or sparsely spiny dendrites (Fig. 7A,C,D,G), characteristic of inhibitory neurons in the cortex (Feldman and Peters 1978; Kawaguchi et al. 2006). Synapses that were not clearly discernible and boutons that appeared to be nonsynaptic varicosities (~17%) were not included in the analysis.

Most postsynaptic targets of axonal boutons from areas 10 and 32 in superior temporal cortex were spines, found on excitatory neurons (from area 10, overall mean = $80 \pm 6\%$ in layers 1–3, $n = 95/114$; from area 32, $86 \pm 10\%$, $n = 62/70$; Fig. 8A,B, white). However, a significant proportion of labeled boutons targeted aspiny or sparsely spiny dendritic shafts (13–18% of all synaptic targets in layers 1–3; Fig. 8A,B, black). The incidence of boutons targeting shafts of spiny dendrites was very low (~1%). A few labeled boutons (~12%) targeted more than one spine, and were included in the analysis.

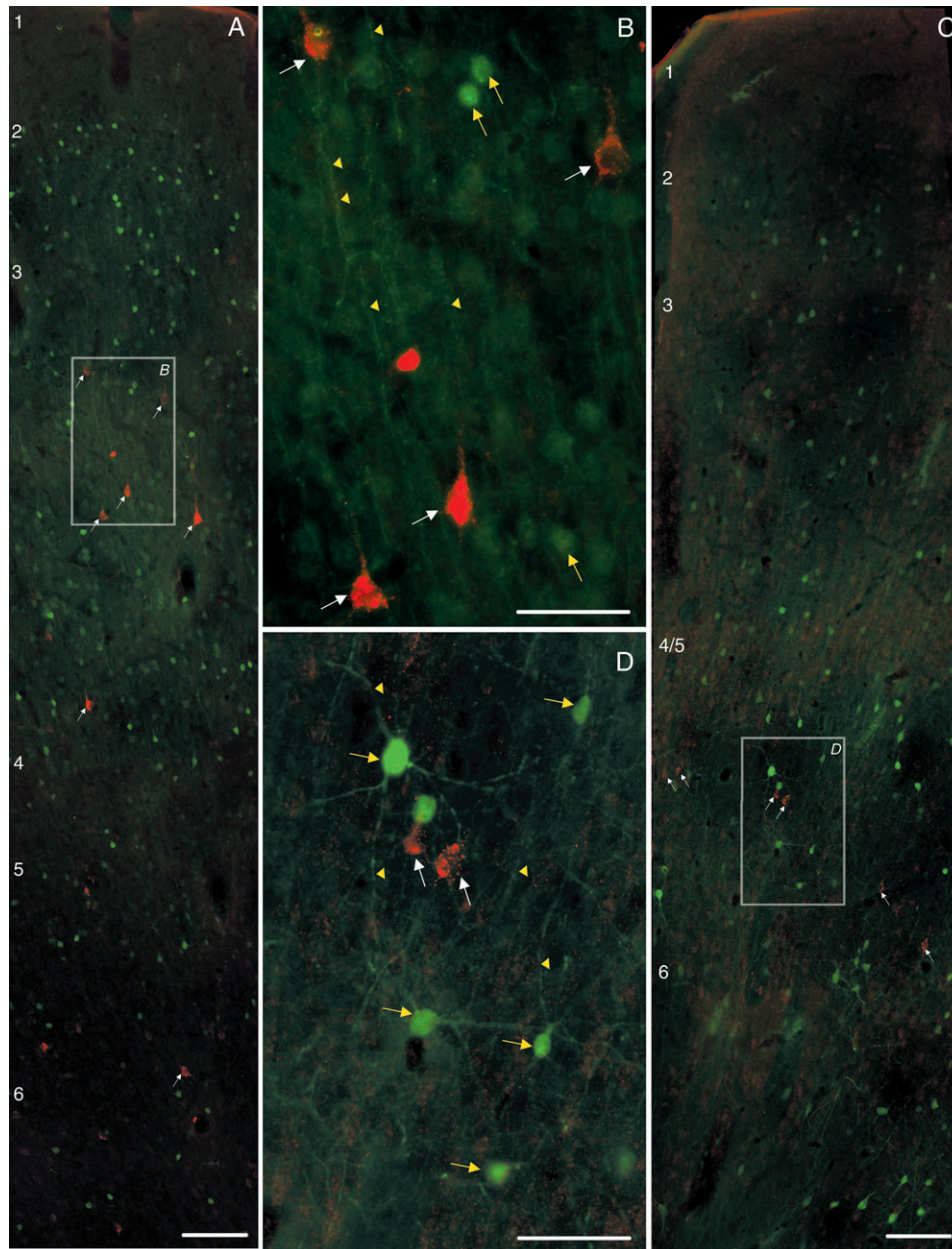


Figure 5. Relationship of prefrontal projection neurons to distinct neurochemical classes of inhibitory neurons. (A) Low power photomicrograph shows labeled projection neurons in area 10 (red, white arrows) that are directed to superior temporal auditory cortices. The FR-labeled projection neurons originated mostly from the upper layers, especially layer 3, and were intermingled with CB inhibitory neurons (green, yellow arrows, and arrowheads), which are prevalent in layers 2-3. (B) Box in A (marked B) is shown at higher magnification. White arrows show FR-labeled projection neurons; yellow arrows show cell bodies of labeled inhibitory neurons; yellow arrowheads show processes of labeled inhibitory neurons. (C) Low power photomicrograph through the anterior cingulate showing labeled neurons in area 32 projecting to superior temporal auditory cortices (red, white arrows). The projection neurons were found predominantly in the deep layers (5-6), and were intermingled mostly with PV inhibitory neurons (green, yellow arrows, and arrowheads). (D) Box from site in C (marked D) is shown at higher magnification. Scale bars: A, C = 100 μ m; B, D = 50 μ m.

Postsynaptic Targets of Prefrontal Axons onto CB+ and PV+ Inhibitory Neurons

Axonal boutons from areas 10 and 32 formed a comparable set of synapses onto excitatory and inhibitory elements that were identified with morphological criteria in superior temporal cortex. However, from the population of synapses onto aspiny dendritic shafts that were labeled with CB or PV, there appeared to be a pathway specific bias, especially in layers 2-3 (Fig. 8C-F). Thus, boutons from area 32 targeted more PV+ shafts of aspiny dendrites (mean = 42% of aspiny targets, $n = 8$; 5% of all targets,

$n = 70$), whereas there was no evidence of synapses with CB+ aspiny dendrites (Fig. 8C,D). In contrast, boutons from area 10 targeted aspiny CB+ (21% of aspiny targets, $n = 10$; 6% of all targets, $n = 56$) and aspiny PV+ dendritic shafts to a similar extent (25% of aspiny targets, $n = 7$; 4% of all targets, $n = 66$; Fig. 8C,D). The preferential targeting was stronger when considering only layers 2-3, where boutons from area 32 targeted mostly PV+ dendrites (67% of aspiny targets; Figs. 7A and 8E, bottom panel), whereas boutons from area 10 targeted a majority of CB+ aspiny dendrites (60%; Figs. 7D and 8F, bottom panel).

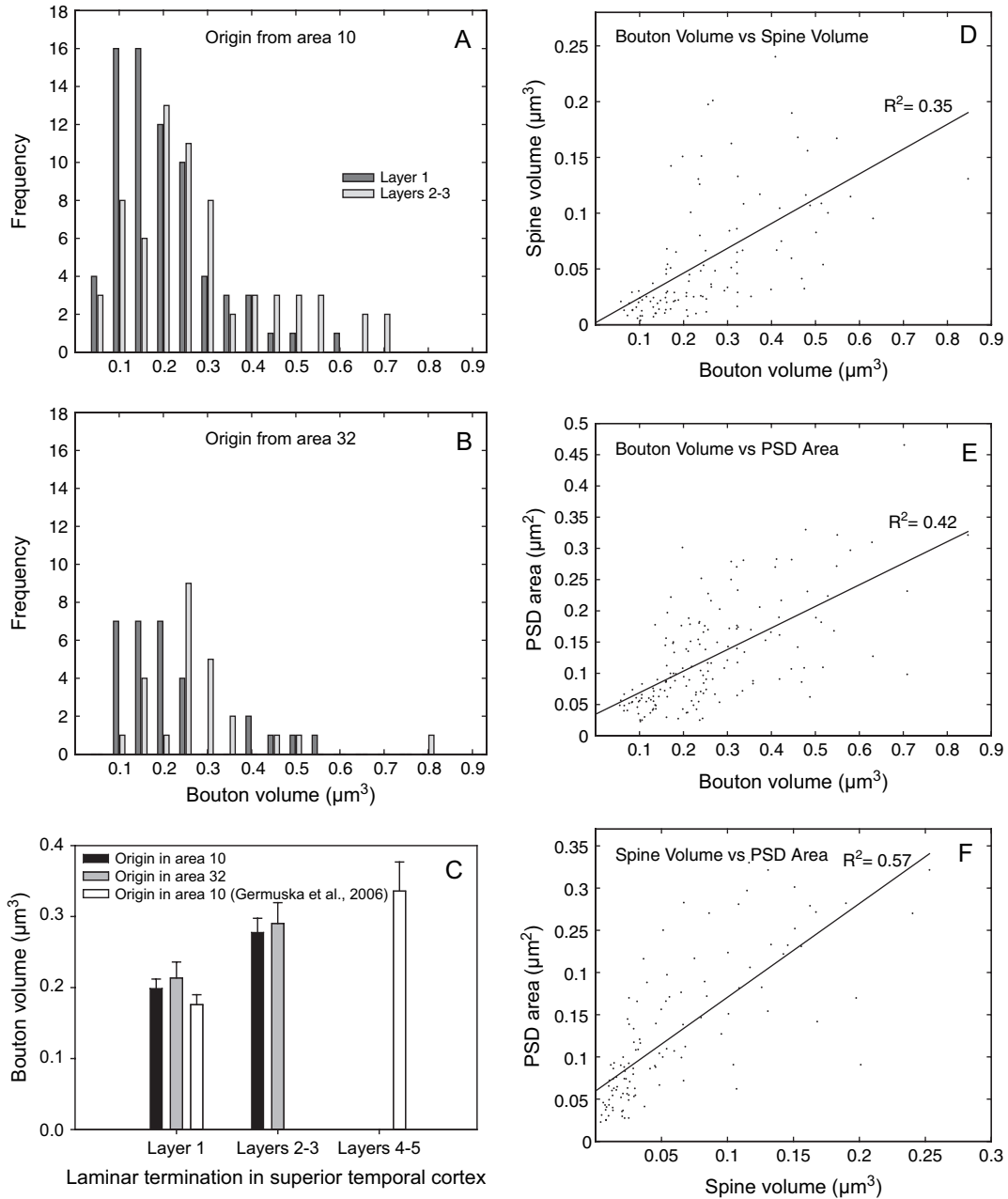


Figure 6. Structural features of synapses linking prefrontal areas with superior temporal cortex. (A, B) Frequency histogram of volumes of boutons (bars) from area 10 (A) and area 32 (B) synapsing in layer 1 (dark gray) and layers 2–3 (light gray) of superior temporal cortex. (C) Average bouton volumes in layer 1 compared with layers 2–3, originating in area 10 (black bars) and area 32 (gray bars) and synapsing in superior temporal cortex. Open bars show volumes in layer 1 and 4–5 from a previous study (Germuska et al. 2006). Vertical lines show standard error. (D) Relationship of spine volume to bouton volume for all cases and layers. (E) Relationship of PSD area to bouton volume for all cases and layers. (F) Relationship of PSD area and spine volume for all cases and layers.

Most inhibitory targets of labeled axonal boutons from both area 10 (77% of aspiny targets; 11% of all targets), and area 32 (58% of aspiny targets; 10% of all targets) were morphologically identified aspiny shafts that were immunonegative (Figs. 7C,G and 8C–F, dark gray), which may be attributed to weak or absent labeling of distal dendrites for CB or PV. This possibility is consistent with the sparse incidence of labeled postsynaptic sites in layer 1 in comparison with layers 2–3, where labeled boutons encounter more proximal dendritic segments (Fig. 8E,F, compare top with bottom panels). The use of serial sections helped identify postsynaptic elements. Beyond the

technical issues, however, it is also possible that unlabeled aspiny dendrites belong to a different neurochemical class of inhibitory neurons, including the class expressing CR, especially in layer 1, where they are prevalent (for review see DeFelipe 1997). Another possibility is that unlabeled aspiny targets may represent the complementary population of CB+ or PV+ interneurons. For example, in temporal tissue that was double labeled to visualize prefrontal terminations and either CB or PV, some unlabeled prefrontal targets found in tissue stained for CB could have been PV+, and vice versa. In the 2 cases with injection of tracer in area 32, however, the tissue was triple labeled (for

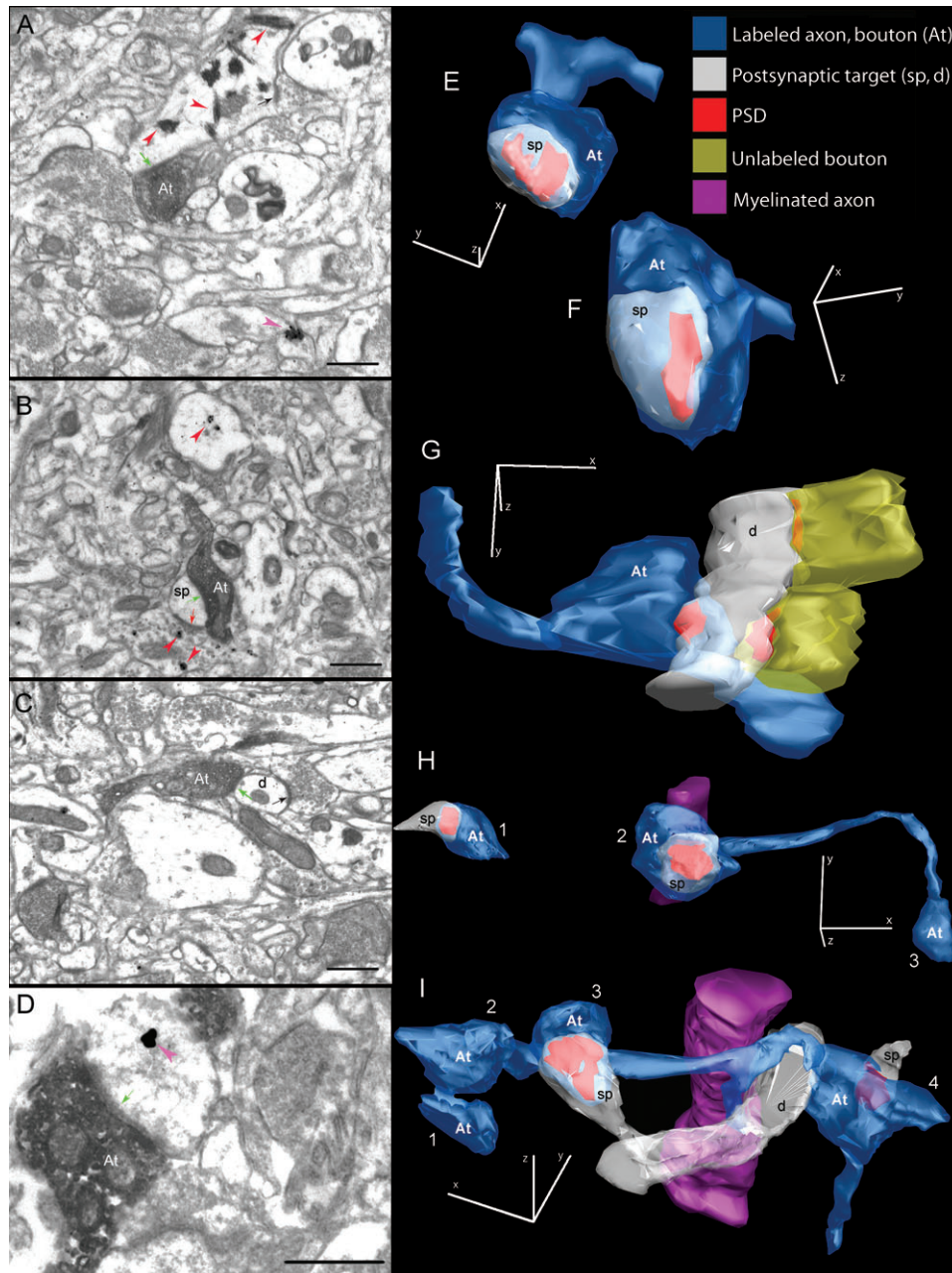


Figure 7. Prefrontal pathways synapsing in superior temporal auditory association cortex. (A) EM photomicrograph showing an FE-labeled bouton from an axon originating in area 32 (At) synapsing (green arrow) in layers 2–3 of temporal auditory area Ts1 on the shaft of a PV+ dendrite labeled with TMB (red arrowheads), which also receives a synapse from an unlabeled bouton (black arrow). Label for CB with gold particles is also seen in the frame (pink arrowhead). (B) EM photomicrograph showing a BDA-labeled bouton from an axon originating in area 32 (At) and synapsing (green arrow) on a spine (sp) in layers 2–3 of area Ts1. The same spine receives a synapse from a PV+ bouton (red arrow) labeled with gold (red arrowheads). (C) EM photomicrograph showing a BDA-labeled bouton from an axon originating in area 32 (At) and terminating in layers 2–3 of area Ts1, synapsing (green arrow) on an aspiny dendrite (d); the latter also receives a synapse from an unlabeled bouton (black arrow). (D) EM photomicrograph showing a BDA-labeled bouton from an axon originating in area 10 (At) and terminating in layers 2–3 of temporal area Ts1, where it synapses (green arrow) on the shaft of a CB+ dendrite labeled with gold (pink arrowhead). (E–I) 3D reconstruction of BDA-labeled boutons from axons originating in prefrontal areas (blue) and terminating in superior temporal cortex, showing: (E) a small bouton from an axon originating in area 10 and terminating in layer 1 of temporal cortex, synapsing on a spine (translucent gray; PSD in red); (F) a large bouton of a prefrontal axon originating in area 10 and terminating in layers 2–3 of temporal cortex, synapsing on a spine; (G) BDA-labeled bouton from an axon originating in area 32 and terminating in layers 2–3 of temporal cortex, where it synapses on the shaft of an aspiny dendrite (d, gray), which also receives 2 additional synapses from unlabeled boutons (yellow). (H) A small FE-labeled axonal bouton from area 32 synapsing on a spine (1) in temporal cortex; a nearby FE-labeled axon has a bouton synapsing on a spine (2), and also has a nonsynaptic bouton (3) in layer 1. (I) An FE-labeled axon from area 32 has 2 nonsynaptic boutons (1 and 2) and 2 boutons (3 and 4) that synapse on spines (gray) in layer 1. Spine shown in 3 emerges from a dendrite (d). Purple in G and I shows the myelinated part of the axon. Scale bars: A–G = 0.5 μ m; H, I = 1.0 μ m.

tracer, CB and PV). In this tissue, labeled boutons from area 32 preferentially targeted PV+ dendrites, even though both CB and PV positive elements were prevalent in the tissue (Fig. 7A). Moreover, in the 2 area 32 injection sites (BI and Ble), we varied

labeling methods for CB and PV (PV labeled with gold and CB with TMB for BI; and the reverse for Ble), but found no synapses with CB+ targets, suggesting that the bias is not due to technical reasons. Even though the numbers of synapses onto aspiny

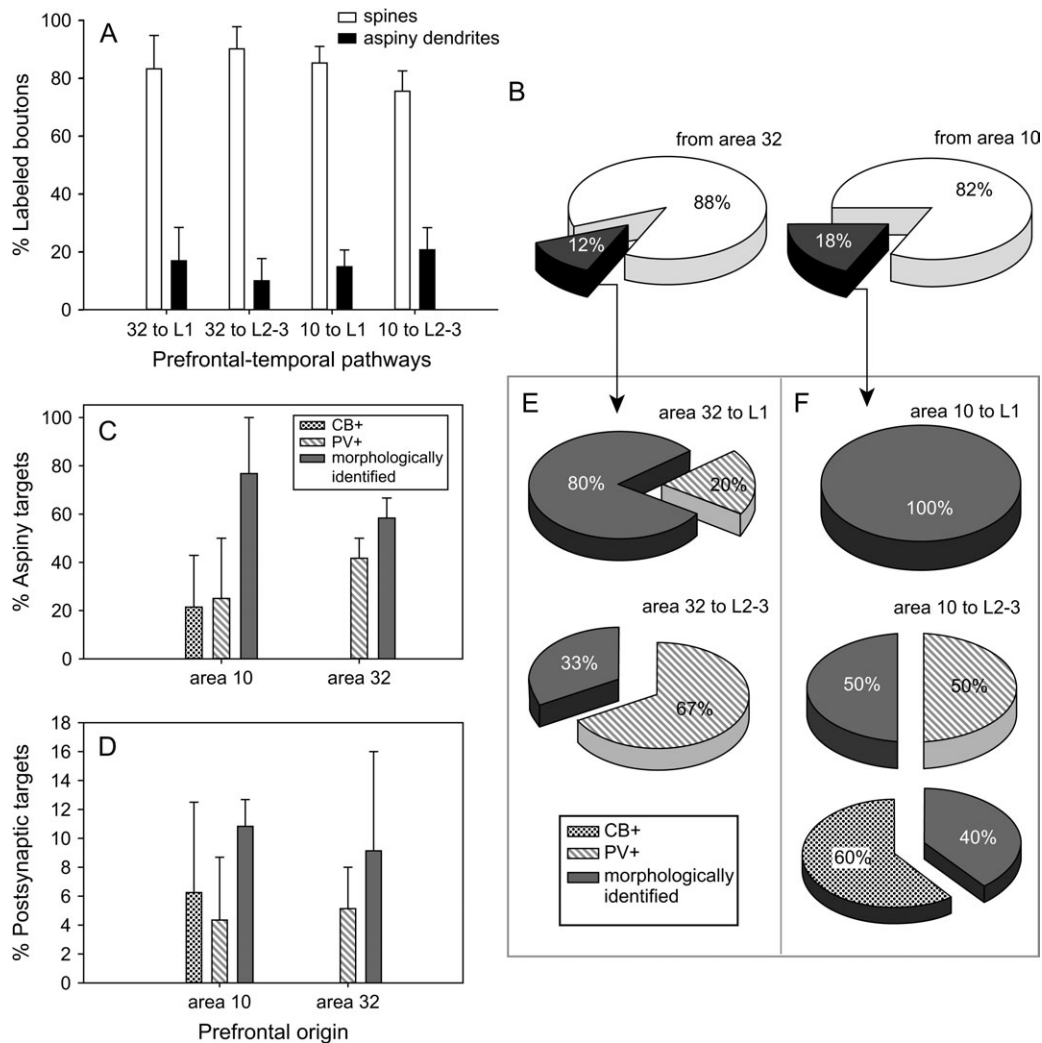


Figure 8. Distribution of labeled boutons from prefrontal axons synapsing on excitatory or inhibitory neuronal elements in superior temporal cortex. (A) Normalized distributions of all labeled boutons synapsing on spines (white) or on shafts of aspiny dendrites (black) in layer 1 (L1) or layers 2–3 (L2–3) from axons originating in prefrontal area 32 (left) and area 10 (right). Vertical lines show standard deviation. (B) Pie chart shows the proportion of labeled boutons from prefrontal axons synapsing with excitatory (white) and inhibitory (black) elements of neurons in superior temporal cortex. (C) Normalized distributions of prefrontal axonal boutons synapsing on elements of inhibitory neurons in superior temporal cortex identified morphologically (dark gray), or by label with CB (dotted pattern) or PV (stripes) are expressed as a proportion of the synapses onto shafts of aspiny dendrites. Vertical lines show standard deviation. (D) Normalized distributions of prefrontal axonal boutons synapsing on elements of inhibitory neurons in superior temporal cortex identified morphologically, or by label with CB or PV are expressed as a proportion of the total postsynaptic targets. Vertical lines show standard deviation. (E) Proportion of synapses made by axonal boutons from area 32 onto elements of inhibitory neurons in superior temporal cortex identified morphologically (dark gray) or by label with PV (stripes) in layer 1 or in layers 2–3. Axons from area 32 synapsed preferentially with PV-labeled dendrites. The tissue was triple-labeled for PV and CB to label inhibitory neurons and BDA or FE to show labeled axonal boutons; no synapses were noted between axonal boutons from area 32 and labeled CB+ inhibitory neurons in superior temporal cortex. (F) Proportion of synapses formed between axons from prefrontal area 10 and elements of inhibitory neurons in superior temporal cortex. Elements of inhibitory neurons were identified morphologically in layer 1 or 2–3 (dark gray) or by PV (stripes) or CB (dotted pattern). All inhibitory synapses in layer 1 were identified by morphologic criteria. In layers 2–3 half of the synapses onto elements of inhibitory neurons were identified by morphologic criteria (dark gray), half by label with PV (stripes, center). In a matched piece of tissue, 60% of synapses on inhibitory neurons were on CB dendritic shafts (dotted pattern, bottom).

labeled dendrites were low, the sample sizes were comparable for all cases examined ($n = 7$ – 10 aspiny dendrites out of 56–70 total boutons per set of immunolabeling).

Finally, there was one instance of a bouton from area 32 that synapsed on a spine in layers 2–3 of superior temporal cortex, and the spine received another synapse from a PV+ bouton (Fig. 7B), suggesting yet another mechanism of inhibition in this corticocortical pathway.

Discussion

Prefrontal areas 32 and 10 provided substantial projections to superior temporal auditory association cortices, confirming

previous findings (Pandya and Kuypers 1969; Jones and Powell 1970; Barbas and Mesulam 1985; Petrides and Pandya 1988; Barbas et al. 1999; Romanski et al. 1999). The 2 prefrontal pathways to auditory association cortex had some features in common, but also differed in significant ways in their association with inhibitory systems, as elaborated below.

Common Features of Prefrontal Pathways to Auditory Association Cortex

The 2 prefrontal pathways innervated mostly spines of excitatory neurons, and synapsed with a comparable and significant proportion of inhibitory neurons in temporal auditory association

cortex. In addition, prefrontal pathways showed a consistent pattern in the size of their terminals that depended on laminar termination in superior temporal cortex. Thus, regardless of their origin in area 32 or area 10, axonal boutons synapsing in layers 2–3 were consistently larger than those synapsing in layer 1. This evidence confirms and extends previous findings (Germuska et al. 2006), and further suggests a graded increase in bouton size from layers 1 to 4–5 in prefrontal to temporal pathways. Moreover, because there is a proportional increase in the number of synaptic vesicles with increase in bouton size (Germuska et al. 2006), and more vesicles are associated with increased probability of multivesicular release of neurotransmitter upon stimulation (Tong and Jahr 1994), these findings suggest that the efficacy of synaptic transmission differs in laminar specific pathways.

Distinct Features of Prefrontal Pathways to Auditory Association Cortices

Beyond the above common features, however, the pathways from the 2 prefrontal areas diverged in significant ways. For example, most temporally directed projection neurons in cingulate area 32 originated in the deep layers (5–6), but in area 10 they were found predominantly in the upper layers (2–3). The sharp laminar differences in these projection neurons place them in distinct laminar microenvironments with respect to neurochemical classes of inhibitory neurons in prefrontal cortices (Dombrowski et al. 2001). Thus, projection neurons from area 10 were intermingled with CB inhibitory neurons, which are most prevalent in layers 2–3 of prefrontal and other cortices (Hendry et al. 1989; Condé et al. 1994; Kondo et al. 1994; Gabbott and Bacon 1996; Glezer et al. 1998; DeFelipe et al. 1999; Dombrowski et al. 2001; Barbas et al. 2005b; Medalla and Barbas 2006). In contrast, projection neurons from area 32 were intermingled with PV inhibitory neurons, which predominate in the middle–deep layers of prefrontal cortices (Dombrowski et al. 2001).

The specific synaptic interactions of projection neurons in areas 32 and 10 with local inhibitory neurons are not known. Previous studies on cortical microcircuitry have shown that pyramidal neurons in the deep and superficial layers interact with both PV+ and CB+ inhibitory neurons (e.g., Melchitzky et al. 1997; Thomson et al. 2002; reviewed in DeFelipe 1997; Kawaguchi and Kubota 1997; Somogyi et al. 1998). However, pyramidal neurons in the upper and deep layers differ in their dendritic arborization, and consequently in their physiological capacity to integrate inputs onto their apical dendritic tufts (e.g., Larkman 1991; Nicoll et al. 1993; Kasper et al. 1994 reviewed in Contreras 2004; Silberberg et al. 2005). Most pyramidal neurons in the upper layers have dense apical tufts that reach layer 1 (Larkman and Mason 1990). On the other hand, some projection neurons in the deep layers, especially those that project to other cortical areas, have apical dendrites that do not arborize as densely or do not extend to layer 1 (e.g., Hallman et al. 1988; Larkman 1991). This evidence suggests that pyramidal neurons in the upper layers may interact more extensively with CB inhibitory neurons, which are concentrated in the upper layers. Double bouquet inhibitory neurons that express CB send narrow descending projections to the deep layers but their axons and processes are densest in layers 2–3 (DeFelipe et al. 1990). Martinotti inhibitory neurons, which are also mostly CB+ in primates, have axons that terminate in

layer 1 and innervate the distal apical tufts of pyramidal neurons (reviewed in DeFelipe 1997; Kawaguchi and Kubota 1997; Thomson and Bannister 2003). In contrast, local inhibitory neurons in the middle layers of the cortex, where PV+ neurons are most prevalent, have axons that rarely extend above layer 3 (reviewed in Thomson and Bannister 2003). Most morphological types of PV+ inhibitory neurons have axons that arborize locally within the vicinity of their cell bodies, or horizontally within the same layers as their somata (reviewed in DeFelipe 1997; Kawaguchi and Kubota 1997; Somogyi et al. 1998). Thus, the PV dominated laminar microenvironment in the middle to deep layers appears to be distinct from the CB rich microenvironment in the upper layers.

Interestingly, prefrontal pathways also showed consistent selectivity in their termination onto distinct classes of inhibitory neurons in temporal cortex. The number of synapses onto labeled neurochemical classes of inhibitory neurons was small but comparable across cases, and showed a consistent trend. Thus, whereas axons from area 10 synapsed with both CB+ and PV+ inhibitory neurons, axons from area 32 targeted PV+ inhibitory neurons. The above evidence suggests that the origin as well as the termination of distinct prefrontal to temporal pathways may differ in their relative interaction with distinct types of inhibitory neurons.

Functional Implications: Diversity in Function of Areas 10 and 32

The 2 prefrontal areas are also functionally diverse. Like other lateral prefrontal areas, area 10 is eulaminate in structure and shares a role in selection and temporary maintenance of task-relevant information in working memory (reviewed in Fuster 2001; Miller and Cohen 2001; Barbas et al. 2002; Petrides 2005). However, area 10 is specifically engaged when a main goal must be kept in mind while temporarily attending to a secondary task (Koechlin et al. 1999; Koechlin et al. 2003). Pathways from area 10 to temporal cortex were associated with both CB and PV inhibitory neurons. In lateral prefrontal cortex, fast-spiking inhibitory neurons, which are thought to express PV, have been implicated in the initial tuning of responses of pyramidal neurons during working memory tasks (Wilson et al. 1994; Rao et al. 1999; Rao et al. 2000; Constantinidis et al. 2002). The interaction of pathways from area 10 to temporal cortex with PV+ inhibitory neurons may play a role in the initial selection of relevant stimuli. On the other hand, CB inhibitory neurons have been implicated in enhancing the signal-to-noise ratio of task-relevant signals and decreasing activity in pyramidal cells carrying task-irrelevant information in working memory tasks (Wang et al. 2004). The unique role of area 10 in maintaining a main goal while temporarily attending to a secondary task may be mediated by modulating irrelevant signals in auditory association cortex through interaction with CB+ inhibitory neurons. Lesions of lateral prefrontal cortex, in general, impair the ability of humans to ignore distracting stimuli, accompanied by increased neural activity in auditory association areas (Knight et al. 1989), suggesting release of inhibitory control by prefrontal cortex (for review see Knight et al. 1999). The impairment in lateral prefrontal function in subjects with attention deficit hyperactivity disorder (for review see Arnsten and Li 2005) may also affect the interaction of prefrontal pathways with CB inhibitory systems.

Previous studies have reported abnormalities in GABAergic neurotransmission in local prefrontal circuits in schizophrenia.

Specifically, there is consensus that CB and PV inhibitory neurons are diminished in lateral prefrontal cortex, especially in the upper layers, accompanied by a compensatory upregulation of GABA receptors and markers of GABAergic neurotransmission (Benes et al. 1991; Beasley and Reynolds 1997; Hashimoto et al. 2003; reviewed in Benes and Berretta 2001; Reynolds et al. 2001; Volk and Lewis 2002). The decrease of both CB and PV mediated inhibition in the upper layers of lateral prefrontal areas may diminish the ability to extract signal from noise, and may help explain the distractibility experienced by schizophrenic patients (reviewed in Cohen et al. 1996).

The pathway from area 32 in the anterior cingulate to auditory association areas provides a distinct example of inhibitory control. When the anterior cingulate cortex is stimulated electrically, auditory evoked activity in superior temporal cortices is reduced (Müller-Preuss et al. 1980; Müller-Preuss and Plog 1981). Functional imaging studies in humans have shown that cognitive tasks involving verbal fluency activate the anterior cingulate and reduce activity in temporal auditory cortices (Dolan et al. 1995; Frith and Dolan 1996). Moreover, the relative activation of anterior cingulate and auditory areas differs when monitoring actual versus inner speech, and these relationships are altered in schizophrenic patients who experience auditory hallucinations (McGuire et al. 1995, 1996; Frith and Dolan 1997). Based on the role of the anterior cingulate cortex in vocalization in emotionally charged circumstances (reviewed in Vogt and Barbas 1988), we have suggested that this area may be involved in emotional communication (Barbas et al. 1999). Specifically, anterior cingulate areas send robust projections that synapse with neurons in hypothalamic autonomic centers (Barbas et al. 2003). The latter innervate peripheral autonomic structures that change their activity during emotional arousal (reviewed in Barbas et al. 2002).

Here we found that most projection neurons in area 32 to auditory association cortex originate in the deep layers. In the brains of schizophrenic patients, PV inhibitory neurons are reported as either increased in density or unchanged in the deep layers (Benes et al. 1992, 1996; Kalus et al. 1997, 1999; Cotter et al. 2002), but pyramidal neurons decrease (Benes et al. 2001). This evidence suggests that in schizophrenia there is reduction in the output from the deep layers of area 32, which likely results in reduced drive onto both excitatory and inhibitory neurons in superior temporal cortex. Hypoactivation in anterior cingulate has been documented in schizophrenic patients, and may affect the ability to distinguish external stimuli from internal thoughts within the auditory domain (McGuire et al. 1996).

Specificity in the Association of Prefrontal Pathways with Inhibitory Systems at their Origin and Termination

Finally, the question arises, does inhibition by prefrontal cortices occur at the level of the prefrontal cortex, or by synapsing of prefrontal axons onto elements of inhibitory neurons in temporal auditory association cortices? The present findings do not distinguish between these possibilities. Further data are necessary to determine whether temporally directed projection neurons in prefrontal cortices are innervated by distinct neurochemical classes of inhibitory neurons, as their laminar origin suggests. Nevertheless, the anatomic specificity of the origin as well as termination of projections from prefrontal to temporal areas suggests that inhibition may be controlled at each end of

these pathways. The preferential association of the prefrontal pathway from area 10 with CB inhibitory neurons at the site of origin and termination may be related to the role of area 10 in juggling multiple tasks within working memory, such as interrupting work on a recipe to answer the phone, before returning to the recipe. Managing both tasks may require temporary modulation of neurons that hold in memory the place of interruption of the recipe, which can then be successfully resumed after answering the phone. CB inhibitory neurons may mediate temporary modulation, consistent with their pattern of innervation of distal dendrites of pyramidal neurons. On the other hand, the association of area 32 with PV neurons, which innervate cell bodies, proximal dendrites, and axon initial segments suggests strong inhibition at the site of origin and termination (reviewed in Kawaguchi and Kubota 1997; Somogyi et al. 1998; Trevelyan and Watkinson 2005) that may prevent a signal from passing on. Cingulate neurons have been associated with monitoring for error and conflict, and respond robustly to commands to reverse a decision for a specific action (Barch et al. 2001; Ito et al. 2003; reviewed in Cohen et al. 2000; Schall et al. 2002), consistent with their association with PV inhibitory neurons. Our findings thus suggest differences in mode of inhibitory control by distinct prefrontal pathways to auditory association cortex. The preferential association of each of these prefrontal pathways with distinct classes of inhibitory neurons may reflect their functional specialization.!

Notes

This paper is dedicated to the memory of Patricia S. Goldman-Rakic. We thank Dr Ron Killiany for assistance with surgery, Dr John Fiala for help with reconstruction, and Dr Basilis Zikopoulos for helpful comments on the manuscript. Supported by NIH grants from the National Institute of Neurological Disorders and Stroke (NINDS) and the National Institute of Mental Health (NIMH). *Conflict of Interest:* None declared.

Address correspondence to Helen Barbas, Boston University, 636 Commonwealth Ave., Room 431, Boston, MA 02215, USA. Email: barbas@bu.edu.

References

- Arnsten AF, Li BM. 2005. Neurobiology of executive functions: catecholamine influences on prefrontal cortical functions. *Biol Psychiatry*. 57:1377-1384.
- Barbas H. 1992. Architecture and cortical connections of the prefrontal cortex in the rhesus monkey. *Adv Neurol*. 57:91-115.
- Barbas H. 1995. Pattern in the cortical distribution of prefrontally directed neurons with divergent axons in the rhesus monkey. *Cereb Cortex*. 5:158-165.
- Barbas H, Ghashghaei H, Dombrowski SM, Rempel-Clower NL. 1999. Medial prefrontal cortices are unified by common connections with superior temporal cortices and distinguished by input from memory-related areas in the rhesus monkey. *J Comp Neurol*. 410:343-367.
- Barbas H, Ghashghaei H, Rempel-Clower N, Xiao D. 2002. Anatomic basis of functional specialization in prefrontal cortices in primates. In: Grafman, J, editor. *Handbook of neuropsychology*. Amsterdam: Elsevier Science B.V. p. 1-27.
- Barbas H, Hilgetag CC, Saha S, Dermon CR, Suski JL. 2005a. Parallel organization of contralateral and ipsilateral prefrontal cortical projections in the rhesus monkey. *BMC Neurosci*. 6:32.
- Barbas H, Medalla M, Alade O, Suski J, Zikopoulos B, Lera P. 2005b. Relationship of prefrontal connections to inhibitory systems in superior temporal areas in the rhesus monkey. *Cereb Cortex*. 15:1356-1370.
- Barbas H, Mesulam MM. 1985. Cortical afferent input to the principal region of the rhesus monkey. *Neuroscience*. 15:619-637.
- Barbas H, Pandya DN. 1989. Architecture and intrinsic connections of the prefrontal cortex in the rhesus monkey. *J Comp Neurol*. 286:353-375.

- Barbas H, Saha S, Rempel-Clower N, Ghashghaei T. 2003. Serial pathways from primate prefrontal cortex to autonomic areas may influence emotional expression. *BMC Neurosci*. 4:25.
- Barch DM, Braver TS, Akbudak E, Conturo T, Ollinger J, Snyder A. 2001. Anterior cingulate cortex and response conflict: effects of response modality and processing domain. *Cereb Cortex*. 11:837-848.
- Beasley CL, Reynolds GP. 1997. Parvalbumin-immunoreactive neurons are reduced in the prefrontal cortex of schizophrenics. *Schizophr Res*. 24:349-355.
- Benes FM, Berretta S. 2001. GABAergic interneurons: implications for understanding schizophrenia and bipolar disorder. *Neuropsychopharmacology*. 25:1-27.
- Benes FM, McSparren J, Bird ED, SanGiovanni JP, Vincent SL. 1991. Deficits in small interneurons in prefrontal and cingulate cortices of schizophrenic and schizoaffective patients. *Arch Gen Psychiatry*. 48:996-1001.
- Benes FM, Vincent SL, Alsterberg G, Bird ED, SanGiovanni JP. 1992. Increased GABA A receptor binding in superficial layers of cingulate cortex in schizophrenics. *J Neurosci*. 12:924-929.
- Benes FM, Vincent SL, Marie A, Khan Y. 1996. Up-regulation of GABA_A receptor binding on neurons of the prefrontal cortex in schizophrenic subjects. *Neuroscience*. 75:1021-1031.
- Benes FM, Vincent SL, Todtenkopf M. 2001. The density of pyramidal and nonpyramidal neurons in anterior cingulate cortex of schizophrenic and bipolar subjects. *Biol Psychiatry*. 50:395-406.
- Chao LL, Knight RT. 1998. Contribution of human prefrontal cortex to delay performance. *J Cogn Neurosci*. 10:167-177.
- Cohen JD, Botvinick M, Carter CS. 2000. Anterior cingulate and prefrontal cortex: who's in control? *Nat Neurosci*. 3:421-423.
- Cohen JD, Braver TS, O'Reilly RC. 1996. A computational approach to prefrontal cortex, cognitive control and schizophrenia: recent developments and current challenges. *Philos Trans R Soc Lond B Biol Sci*. 351:1515-1527.
- Condé F, Lund JS, Jacobowitz DM, Baimbridge KG, Lewis DA. 1994. Local circuit neurons immunoreactive for calretinin, calbindin D-28k or parvalbumin in monkey prefrontal cortex: distribution and morphology. *J Comp Neurol*. 341:95-116.
- Constantinidis C, Franowicz MN, Goldman-Rakic PS. 2001. Coding specificity in cortical microcircuits: a multiple-electrode analysis of primate prefrontal cortex. *J Neurosci*. 21:3646-3655.
- Constantinidis C, Williams GV, Goldman-Rakic PS. 2002. A role for inhibition in shaping the temporal flow of information in prefrontal cortex. *Nat Neurosci*. 5:175-180.
- Contreras D. 2004. Electrophysiological classes of neocortical neurons. *Neural Netw*. 17:633-646.
- Cotter D, Landau S, Beasley C, Stevenson R, Chana G, MacMillan L, Everall I. 2002. The density and spatial distribution of GABAergic neurons, labelled using calcium binding proteins, in the anterior cingulate cortex in major depressive disorder, bipolar disorder, and schizophrenia. *Biol Psychiatry*. 51:377-386.
- Dagenbach D, Carr TH. 1994. Inhibitory processes in attention, memory, and language. San Diego: Academic Press.
- DeFelipe J. 1997. Types of neurons, synaptic connections and chemical characteristics of cells immunoreactive for calbindin-D28K, parvalbumin and calretinin in the neocortex. *J Chem Neuroanat*. 14:1-19.
- DeFelipe J, Gonzalez-Albo MC, del Rio MR, Elston GN. 1999. Distribution and patterns of connectivity of interneurons containing calbindin, calretinin, and parvalbumin in visual areas of the occipital and temporal lobes of the macaque monkey. *J Comp Neurol*. 412: 515-526.
- DeFelipe J, Hendry SH, Hashikawa T, Molinari M, Jones EG. 1990. A microcolumnar structure of monkey cerebral cortex revealed by immunocytochemical studies of double bouquet cell axons. *Neuroscience*. 37:655-673.
- DeFelipe J, Hendry SH, Jones EG. 1989a. Synapses of double bouquet cells in monkey cerebral cortex visualized by calbindin immunoreactivity. *Brain Res*. 503:49-54.
- DeFelipe J, Hendry SH, Jones EG. 1989b. Visualization of chandelier cell axons by parvalbumin immunoreactivity in monkey cerebral cortex. *Proc Natl Acad Sci USA*. 86:2093-2097.
- Dolan RJ, Fletcher P, Frith CD, Friston KJ, Frackowiak RSJ, Grasby PM. 1995. Dopaminergic modulation of impaired cognitive activation in the anterior cingulate cortex in schizophrenia. *Nature*. 378: 180-182.
- Dombrowski SM, Hilgetag CC, Barbas H. 2001. Quantitative architecture distinguishes prefrontal cortical systems in the rhesus monkey. *Cereb Cortex*. 11:975-988.
- Feldman ML, Peters A. 1978. The forms of non-pyramidal neurons in the visual cortex of the rat. *J Comp Neurol*. 179:761-793.
- Fiala JC. 2005. Reconstruct: a free editor for serial section microscopy. *J Microsc*. 218:52-61.
- Fiala JC, Harris KM. 2001. Cylindrical diameters method for calibrating section thickness in serial electron microscopy. *J Microsc*. 202: 468-472.
- Fiala JC, Harris KM. 2002. Computer-based alignment and reconstruction of serial sections. *Microsc Anal USA Ed*. 52:5-7.
- Frith C, Dolan R. 1996. The role of the prefrontal cortex in higher cognitive functions. *Brain Res Cogn Brain Res*. 5:175-181.
- Frith CD, Dolan RJ. 1997. Brain mechanisms associated with top-down processes in perception. *Philos Trans R Soc Lond B Biol Sci*. 352: 1221-1230.
- Fuster JM. 2001. The prefrontal cortex—an update: time is of the essence. *Neuron*. 30:319-333.
- Gabbott PL, Bacon SJ. 1996. Local circuit neurons in the medial prefrontal cortex (areas 24a,b,c, 25 and 32) in the monkey: II. Quantitative areal and laminar distributions. *J Comp Neurol*. 364: 609-636.
- Germuska M, Saha S, Fiala J, Barbas H. 2006. Synaptic distinction of laminar specific prefrontal-temporal pathways in primates. *Cereb Cortex*. 16:865-875.
- Giberson RT, Elliott DE. 2001. Microwave-assisted formalin fixation of fresh tissue: a comparative study. In: Giberson RT, Demaree RS, editors. *Microwave techniques and protocols*. Totowa: Humana Press, Inc. p. 191-208.
- Glezer II, Hof PR, Morgane PJ. 1998. Comparative analysis of calcium-binding protein-immunoreactive neuronal populations in the auditory and visual systems of the bottlenose dolphin (*Tursiops truncatus*) and the macaque monkey (*Macaca fascicularis*). *J Chem Neuroanat*. 15:203-237.
- Gonchar Y, Burkhalter A. 1999. Connectivity of GABAergic calretinin-immunoreactive neurons in rat primary visual cortex. *Cereb Cortex*. 9:683-696.
- Gonchar Y, Burkhalter A. 2003. Distinct GABAergic targets of feedforward and feedback connections between lower and higher areas of rat visual cortex. *J Neurosci*. 23:10904-10912.
- Gupta A, Wang Y, Markram H. 2000. Organizing principles for a diversity of GABAergic interneurons and synapses in the neocortex. *Science*. 287:273-278.
- Hackett TA, Stepniewska I, Kaas JH. 1999. Prefrontal connections of the parabelt auditory cortex in macaque monkeys. *Brain Res*. 817:45-58.
- Hallman LE, Schofield BR, Lin CS. 1988. Dendritic morphology and axon collaterals of corticotectal, corticopontine, and callosal neurons in layer V of primary visual cortex of the hooded rat. *J Comp Neurol*. 272:149-160.
- Hashimoto T, Volk DW, Eggan SM, Mirnics K, Pierri JN, Sun Z, Sampson AR, Lewis DA. 2003. Gene expression deficits in a subclass of GABA neurons in the prefrontal cortex of subjects with schizophrenia. *J Neurosci*. 23:6315-6326.
- Hendry SH, Jones EG, Emson PC, Lawson DEM, Heizmann CW, Streit P. 1989. Two classes of cortical GABA neurons defined by differential calcium binding protein immunoreactivities. *Exp Brain Res*. 76: 467-472.
- Ito S, Stuphorn V, Brown JW, Schall JD. 2003. Performance monitoring by the anterior cingulate cortex during saccade countermanding. *Science*. 302:120-122.
- Jensen FE, Harris KM. 1989. Preservation of neuronal ultrastructure in hippocampal slices using rapid microwave-enhanced fixation. *J Neurosci Methods*. 29:217-230.
- Jones EG, Powell TPS. 1970. An anatomical study of converging sensory pathways within the cerebral cortex. *Brain*. 93:793-820.

- Kalus P, Senitz D, Beckmann H. 1997. Altered distribution of parvalbumin-immunoreactive local circuit neurons in the anterior cingulate cortex of schizophrenic patients. *Psychiatr Res.* 75:49-59.
- Kalus P, Senitz D, Lauer M, Beckmann H. 1999. Inhibitory cartridge synapses in the anterior cingulate cortex of schizophrenics. *J Neural Transm.* 106:763-771.
- Kasper EM, Larkman AU, Lubke J, Blakemore C. 1994. Pyramidal neurons in layer 5 of the rat visual cortex. I. Correlation among cell morphology, intrinsic electrophysiological properties, and axon targets. *J Comp Neurol.* 339:459-474.
- Kawaguchi Y, Karube F, Kubota Y. 2006. Dendritic branch typing and spine expression patterns in cortical nonpyramidal cells. *Cereb Cortex.* 16:696-711.
- Kawaguchi Y, Kubota Y. 1997. GABAergic cell subtypes and their synaptic connections in rat frontal cortex. *Cereb Cortex.* 7:476-486.
- Knight RT, Scabini D, Woods DL. 1989. Prefrontal cortex gating of auditory transmission in humans. *Brain Res.* 504:338-342.
- Knight RT, Staines WR, Swick D, Chao LL. 1999. Prefrontal cortex regulates inhibition and excitation in distributed neural networks. *Acta Psychol (Amst).* 101:159-178.
- Koechlin E, Basso G, Pietrini P, Panzer S, Grafman J. 1999. The role of the anterior prefrontal cortex in human cognition. *Nature.* 399:148-151.
- Koechlin E, Ody C, Kouneiher F. 2003. The architecture of cognitive control in the human prefrontal cortex. *Science.* 302:1181-1185.
- Kondo H, Hashikawa T, Tanaka K, Jones EG. 1994. Neurochemical gradient along the monkey occipito-temporal cortical pathway. *NeuroReport.* 5:613-616.
- Krimer LS, Goldman-Rakic PS. 2001. Prefrontal microcircuits: membrane properties and excitatory input of local, medium, and wide arbor interneurons. *J Neurosci.* 21:3788-3796.
- Kritzer MF, Cowey A, Somogyi P. 1992. Patterns of inter- and intralaminar GABAergic connections distinguish striate (V1) and extrastriate (V2, V4) visual cortices and their functionally specialized subdivisions in the rhesus monkey. *J Neurosci.* 12:4545-4564.
- Larkman A, Mason A. 1990. Correlations between morphology and electrophysiology of pyramidal neurons in slices of rat visual cortex. I. Establishment of cell classes. *J Neurosci.* 10:1407-1414.
- Larkman AU. 1991. Dendritic morphology of pyramidal neurons of the visual cortex of the rat: I. Branching patterns. *J Comp Neurol.* 306:307-319.
- McGuire PK, Silbersweig DA, Wright I, Murray RM, David AS, Frackowiak RSJ, Frith CD. 1995. Abnormal monitoring of inner speech: a physiological basis for auditory hallucinations. *Lancet.* 346:596-600.
- McGuire PK, Silbersweig DA, Wright I, Murray RM, Frackowiak RSJ, Frith CD. 1996. The neural correlates of inner speech and auditory verbal imagery in schizophrenia: relationship to auditory verbal hallucinations. *Br J Psychiatry.* 169:148-159.
- Medalla M, Barbas H. 2006. Diversity of laminar connections linking periarculate and lateral intraparietal areas depends on cortical structure. *Eur J Neurosci.* 23:161-179.
- Melchitzky DS, Eggen SM, Lewis DA. 2005. Synaptic targets of calretinin-containing axon terminals in macaque monkey prefrontal cortex. *Neuroscience.* 130:185-195.
- Melchitzky DS, Sesack SR, Lewis DA. 1997. Axosomatic input to subpopulations of cortically projecting pyramidal neurons in primate prefrontal cortex. *Synapse.* 25:326-334.
- Melchitzky DS, Sesack SR, Pucak ML, Lewis DA. 1998. Synaptic targets of pyramidal neurons providing intrinsic horizontal connections in monkey prefrontal cortex. *J Comp Neurol.* 390:211-224.
- Meskenaite V. 1997. Calretinin-immunoreactive local circuit neurons in area 17 of the cynomolgus monkey, *Macaca fascicularis*. *J Comp Neurol.* 379:113-132.
- Miller EK, Cohen JD. 2001. An integrative theory of prefrontal cortex function. *Annu Rev Neurosci.* 24:167-202.
- Moore CT, Wilson CG, Mayer CA, Acquah SS, Massari VJ, Haxhiu MA. 2004. A GABAergic inhibitory microcircuit controlling cholinergic outflow to the airways. *J Appl Physiol.* 96:260-270.
- Müller-Preuss JD, Newman JD, Jürgens U. 1980. Anatomical and physiological evidence for a relationship between the 'cingular' vocalization area and the auditory cortex in the squirrel monkey. *Brain Res.* 202:307-315.
- Müller-Preuss P, Ploog D. 1981. Inhibition of auditory cortical neurons during phonation. *Brain Res.* 215:61-76.
- Nicoll A, Larkman A, Blakemore C. 1993. Modulation of EPSP shape and efficacy by intrinsic membrane conductances in rat neocortical pyramidal neurons in vitro. *J Physiol.* 468:693-710.
- Pandya DN, Kuypers HGJM. 1969. Cortico-cortical connections in the rhesus monkey. *Brain Res.* 13:13-36.
- Paus T. 2001. Primate anterior cingulate cortex: where motor control, drive and cognition interface. *Nat Rev Neurosci.* 2:417-424.
- Peters A, Palay SL, Webster HD. 1991. The fine structure of the nervous system. Neurons and their supporting cells. New York: Oxford University Press.
- Peters A, Sethares C. 1997. The organization of double bouquet cells in monkey striate cortex. *J Neurocytol.* 26:779-797.
- Petrides M. 2005. Lateral prefrontal cortex: architectonic and functional organization. *Philos Trans R Soc Lond B Biol Sci.* 360:781-795.
- Petrides M, Pandya DN. 1988. Association fiber pathways to the frontal cortex from the superior temporal region in the rhesus monkey. *J Comp Neurol.* 273:52-66.
- Posner MI, DiGirolamo GJ. 1998. Executive attention: conflict, target detection, and cognitive control. In: Parasuraman, R, editor. *The attentive brain*. Cambridge (MA): The MIT Press. p. 401-423.
- Rao SG, Williams GV, Goldman-Rakic PS. 1999. Isodirectional tuning of adjacent interneurons and pyramidal cells during working memory: evidence for microcolumnar organization in PFC. *J Neurophysiol.* 81:1903-1916.
- Rao SG, Williams GV, Goldman-Rakic PS. 2000. Destruction and creation of spatial tuning by disinhibition: GABA(A) blockade of prefrontal cortical neurons engaged by working memory. *J Neurosci.* 20:485-494.
- Reiner A, Veenman CL, Medina L, Jiao Y, Del Mar N, Honig MG. 2000. Pathway tracing using biotinylated dextran amines. *J Neurosci Methods.* 103:23-37.
- Reynolds GP, Zhang ZJ, Beasley CL. 2001. Neurochemical correlates of cortical GABAergic deficits in schizophrenia: selective losses of calcium binding protein immunoreactivity. *Brain Res Bull.* 55:579-584.
- Romanski LM, Bates JF, Goldman-Rakic PS. 1999. Auditory belt and parabelt projections to the prefrontal cortex in the rhesus monkey. *J Comp Neurol.* 403:141-157.
- Rosene DL, Roy NJ, Davis BJ. 1986. A cryoprotection method that facilitates cutting frozen sections of whole monkey brains from histological and histochemical processing without freezing artifact. *J Histochem Cytochem.* 34:1301-1315.
- Schall JD, Stuphorn V, Brown JW. 2002. Monitoring and control of action by the frontal lobes. *Neuron.* 36:309-322.
- Silberberg G, Grillner S, LeBeau FE, Maex R, Markram H. 2005. Synaptic pathways in neural microcircuits. *Trends Neurosci.* 28:541-551.
- Somogyi P, Kisvarday ZF, Martin KA, Whitteridge D. 1983. Synaptic connections of morphologically identified and physiologically characterized large basket cells in the striate cortex of cat. *Neuroscience.* 10:261-294.
- Somogyi P, Tamas G, Lujan R, Buhl EH. 1998. Salient features of synaptic organization in the cerebral cortex. *Brain Res Brain Res Rev.* 26:113-135.
- Thomson AM, Bannister AP. 2003. Interlaminar connections in the neocortex. *Cereb Cortex.* 13:5-14.
- Thomson AM, Deuchars J. 1997. Synaptic interactions in neocortical local circuits: dual intracellular recordings in vitro. *Cereb Cortex.* 7:510-522.
- Thomson AM, West DC, Wang Y, Bannister AP. 2002. Synaptic connections and small circuits involving excitatory and inhibitory neurons in layers 2-5 of adult rat and cat neocortex: triple intracellular recordings and biocytin labelling in vitro. *Cereb Cortex.* 12:936-953.
- Tong G, Jahr CE. 1994. Multivesicular release from excitatory synapses of cultured hippocampal neurons. *Neuron.* 12:51-59.
- Trevelyan AJ, Watkinson O. 2005. Does inhibition balance excitation in neocortex? *Prog Biophys Mol Biol.* 87:109-143.

- Veenman CL, Reiner A, Honig MG. 1992. Biotinylated dextran amine as an anterograde tracer for single- and double-labeling studies. *J Neurosci Methods*. 41:239-254.
- Vogt BA, Barbas H. 1988. Structure and connections of the cingulate vocalization region in the rhesus monkey. In: Newman, JD, editor. *The physiological control of mammalian vocalization*. New York: Plenum Publ. Corp. p. 203-225.
- Volk DW, Lewis DA. 2002. Impaired prefrontal inhibition in schizophrenia: relevance for cognitive dysfunction. *Physiol Behav*. 77:501-505.
- Wang XJ, Tegner J, Constantinidis C, Goldman-Rakic PS. 2004. Division of labor among distinct subtypes of inhibitory neurons in a cortical microcircuit of working memory. *Proc Natl Acad Sci USA*. 101:1368-1373.
- White EL, Keller A. 1989. *Cortical circuits. Synaptic organization of the cerebral cortex. Structure, function and theory*. Boston: Birkhäuser.
- Wilson FA, O'Scalaidhe SP, Goldman-Rakic PS. 1994. Functional synergism between putative gamma-aminobutyrate-containing neurons and pyramidal neurons in prefrontal cortex. *Proc Natl Acad Sci USA*. 91:4009-4013.
- Woods DL, Knight RT. 1986. Electrophysiologic evidence of increased distractibility after dorsolateral prefrontal lesions. *Neurology*. 36:212-216.
- Zaitsev A, Gonzalez-Burgos G, Povysheva N, Kroner S, Lewis D, Krimer L. 2005. Localization of calcium-binding proteins in physiologically and morphologically characterized interneurons of monkey dorsolateral prefrontal cortex. *Cereb Cortex*. 15:1178-1186.
- Zikopoulos B, Barbas H. 2006. Prefrontal projections to the thalamic reticular nucleus form a unique circuit for attentional mechanisms. *J Neurosci*. 26:7348-7361.